



## SITE RESPONSE IMPLICATINS OF USING $V_s$ PROFILES DERIVED FROM “BLIND” AND GEOLOGICALLY-GUIDED SURFACE WAVE INVERSIONS

D.P. Teague<sup>(1)</sup>, B.R. Cox<sup>(2)</sup>, T. El-Afifi<sup>(3)</sup>

<sup>(1)</sup> PhD Candidate, The University of Texas at Austin, [dteague@utexas.edu](mailto:dteague@utexas.edu)

<sup>(2)</sup> Associate Professor, The University of Texas at Austin, [brcox@utexas.edu](mailto:brcox@utexas.edu)

<sup>(3)</sup> Undergraduate Research Assistant, The University of Texas at Austin, [telafifi@utexas.edu](mailto:telafifi@utexas.edu)

### **Abstract**

Linear-elastic (LE) and equivalent-linear (EQL) site response analyses were performed on two unique sets of  $V_s$  profiles, both of which were derived from the same surface wave data measured at Hagley Park in Christchurch, New Zealand. The first set of  $V_s$  profiles, Analysis 1, was developed using normally dispersive inversion parameters and did not account for the complex local geology. The second set of  $V_s$  profiles, Analysis 2, incorporated strong velocity reversals in the inversion parameters where marine sands, silts, and clays were known to reside below stiffer alluvial gravels. The influence of the presence or lack of velocity reversals on the predicted site response is considered. Fifty  $V_s$  profiles from each analysis whose theoretical dispersion curves matched the experimental dispersion data approximately equally-well were sampled and used in LE and EQL site response calculations. Overall, LE and EQL site response predictions for Analyses 1 and 2 were quite similar. This suggests that despite major differences in the input  $V_s$  profiles, those  $V_s$  profiles with similar dispersion misfit values exhibit similar site response. Additionally, median and “bounding-type” statistical  $V_s$  profiles (i.e., the median  $V_s$  profile  $\pm 20\%$ ) were considered. The theoretical dispersion curve derived from the median  $V_s$  profile fit the experimental dispersion data well and the LE and EQL site response were in satisfactory agreement with results from the inversion  $V_s$  profiles. However, theoretical dispersion curves derived from the  $\pm 20\%$   $V_s$  profile did not fit the experimental dispersion data well and the site response results were outliers relative to the other  $V_s$  profiles, with the differences becoming more pronounced with ground motion intensity.

*Keywords: shear wave velocity, surface wave inversion, inversion parameterization, a-priori information, site response*



## 1. Introduction

The input shear wave velocity ( $V_s$ ) profile has been shown to significantly influence the results of a site response analysis. Both epistemic uncertainty and aleatory variability are inherent in the input  $V_s$  profile and this uncertainty/variability translates to uncertainty in the predicted site response. While engineering design codes emphasize the importance of accounting for  $V_s$  uncertainty (e.g., ASCE 2010 [1], AASHTO 2011 [2]), no firm guidelines are provided and numerous approaches are utilized in practice (Matasovic and Hashash 2012 [3]).

While  $V_s$  profiles are commonly measured using invasive borehole methods (i.e., seismic crosshole, seismic downhole, and PS suspension logging), non-invasive surface wave methods offer an efficient and cost-effective alternative. Surface wave methods involve finding layered earth models whose forward-computed theoretical dispersion curves acceptably match an experimental dispersion curve derived from field measurements. Layered earth models comprise a system of stacked, linear-elastic layers, each defined by its thickness,  $V_s$ , compression wave velocity ( $V_p$ ) or Poisson's ratio, and mass density. For earthquake engineering purposes, thickness and  $V_s$  are of primary interest. A major criticism of surface wave methods is the ill-posed nature of the inverse problem and the resulting non-uniqueness of the final  $V_s$  profiles. Indeed, it is possible to find significantly different  $V_s$  profiles whose theoretical dispersion curves match the experimental data equally well. Prior studies have demonstrated that the parameterization used in the inversion (i.e., trial number of layers and ranges in their respective depths/thicknesses,  $V_s$ ,  $V_p$ , and mass densities) drastically influence the resulting  $V_s$  profiles (DiGiulio et al. 2012 [4], Cox and Teague 2016 [5]). Cox and Teague (2016) [5] show that the number of trial layers is particularly important, with too many layers resulting in  $V_s$  profiles that are overly "smooth" and fail to capture strong velocity contrasts and too few layers resulting in  $V_s$  profiles that place strong velocity contrasts at incorrect depths. In situations when no a-priori information is available, they propose conducting multiple inversions utilizing systematically-varied inversion layering parameterizations in order to identify and encompass the most reasonable layered earth models for a site. However, even when such an approach is utilized, there are many real sites where significantly different  $V_s$  profiles may be deemed acceptable and the influence of this non-uniqueness (i.e., uncertainty) on the predicted site response is of great interest.

Several studies have investigated the variability in site response estimates derived from non-unique  $V_s$  profiles obtained via surface wave testing (e.g., Foti et al. 2009 [6], Boaga et al. 2011 [7], Griffiths et al. 2016b [8], Teague and Cox 2016 [9]). A detailed review of these studies is beyond the scope of this paper, however, the reader is referred to Teague and Cox (2016) [9] for a brief overview. Recently, Teague and Cox (2016) [9] performed linear elastic (LE) and equivalent-linear (EQL) site response analyses on 350  $V_s$  profiles from their original study, which were derived from systematically-varied inversion layering parameterizations. They found that despite significant differences in the  $V_s$  profiles, so long as their theoretical dispersion data fit the experimental dispersion data well, their dispersion misfit-weighted site response results were quite accurate with minimal variability. Furthermore, the site response estimates associated with  $V_s$  profiles derived from surface wave inversions were significantly more accurate and exhibited less variability than profiles derived using other common methods of accounting for  $V_s$  uncertainty, such as the use of bounding-type and statistically-based, randomly-generated  $V_s$  profiles.

While the previous studies provide valuable insight regarding the influence of  $V_s$  uncertainty on the predicted site response, further investigation is required. In the previously mentioned studies, those  $V_s$  profiles whose theoretical dispersion curves satisfactorily fit the experimental dispersion data were normally dispersive (i.e.,  $V_s$  increasing with depth) or contained only minor velocity reversals (i.e., when the  $V_s$  of a layer is lower than that of the overlying layer). However, large velocity reversals exist in many geologic environments. Moreover, in many situations it is possible to fit the experimental dispersion data equally well by performing an inversion using either a normally dispersive inversion parameterization or one that incorporates strong velocity reversals. In order to investigate this topic, site response analyses were conducted on  $V_s$  profiles developed at Hagley Park in Christchurch, New Zealand, where the geology is expected to include large velocity reversals.



## 2. Vs Profiles Developed at Hagley Park

Hagley Park is located on the deep soils of the Canterbury Plains, whose geology consists primarily of alluvial gravels inter-bedded with formations of estuarine and marine sands, silts, clays, and peats (Brown et al. 1988 [10]). Teague et al. (2015) [11] performed inversions on an extensive active-source and passive-wavefield surface wave dataset collected at the Hagley Park site using both a simple normally dispersive inversion parameterization and a parameterization that accounted for the complex local geology with multiple strong velocity reversals. These inversions are referred to as Analyses 1 and 2, respectively. The reader is referred to Teague et al. (2015) [11] for detailed discussion of the field acquisition, dispersion processing, and inversion procedures.

While Teague et al. (2015) [11] consider the 1,000 lowest misfit Vs profiles derived from each inversion analysis in their study, it would be too computationally expensive to perform site response calculations on 1,000 Vs profiles from each analysis. Therefore, 50 Vs profiles were randomly sampled from the 1,000 lowest misfit profiles from Analyses 1 and 2. A median and coefficient of variation profile were computed for both the 50 and 1,000 profiles and found to be essentially equal, indicating that the 50 profiles are a representative sample of the 1,000. Fig. 1 shows the fifty Vs profiles from each analysis. All Vs profiles were truncated at the first layer exceeding 700 m/s because the input ground motions for this study were selected using a target response spectrum with a  $V_{S30}$  of 760 m/s. Also shown in Fig. 1 is the approximate geologic stratigraphy, which was used to constrain the inversion parameters for Analysis 2.

It is clear from Fig. 1 that the Vs profiles from Analyses 1 and 2 are quite different. Analysis 2 is more consistent with the a-priori geologic data, as it includes velocity reversals where a geologic formation comprised of sand, silt, or clay underlines a geologic formation comprised of gravel. This is to be expected because gravels are generally stiffer than sands, silts, or clays for a given confining pressure. Moreover, the empirical soil-type reference curves from Lin et al. (2014) [12] show that the Vs profiles from Analysis 2 are consistent with the known material types. Conversely, Vs profiles from Analysis 1 simply average material types as a function of depth and generally lie between the reference curves for dense sand and dense gravel. This is because information about the local geology was not used to constrain the inversion parameters for Analysis 1. Therefore, the results from Analysis 1 could be obtained without any a-priori information, while it would be nearly impossible to obtain the Vs profiles from Analysis 2 without geologic and/or borehole data to constrain the inversion parameters.

Fig. 2 shows the experimental dispersion data along with the theoretical dispersion data corresponding to the 50 Vs profiles derived directly from the inversions (termed “inversion profiles”). While the differences between Vs profiles from Analyses 1 and 2 are pronounced, it is clear from Fig. 2 that both analyses result in similar fits of the experimental dispersion data. In both cases, data between 2 and 4 Hz were fit with the first higher Rayleigh mode (orange or cyan theoretical dispersion curves), while data at all other frequencies were fit with the fundamental mode (red or green theoretical dispersion curves). Note that the experimental dispersion data between 1 and 2 Hz was eliminated because it was deemed to represent an effective mode, which could not be accounted for in the multi-mode inversion used in this study. Dispersion misfit values are shown in brackets. Note that a lower misfit value indicates a better match between the experimental and theoretical dispersion curves. The ranges in dispersion misfit for both analyses are 0.62 to 0.75 and 0.68 to 0.80, respectively. Thus, the theoretical dispersion curves corresponding to the inversion profiles from Analyses 1 and 2 fit the experimental data approximately equally well. This underscores the non-uniqueness of the surface wave inverse problem. Since Vs profiles derived from surface wave analyses are often used in site response analyses, it is important to consider how the presence or lack of velocity reversals and strong impedance contrasts influences the predicted site response.

The median profile and “bounding-type” profiles, which were developed by applying +/-20% to the median Vs profile, are shown for each analysis in Fig. 1. These Vs profiles are considered because a median Vs profile is often used as a “best” estimate and bounding-type profiles are often used to account for epistemic uncertainty (Griffiths et al. 2016a [13]). Fig. 2 shows the theoretical dispersion data for the median and +/-20% profiles. It should be noted that these profiles were not derived directly from the inversion. Rather, they were

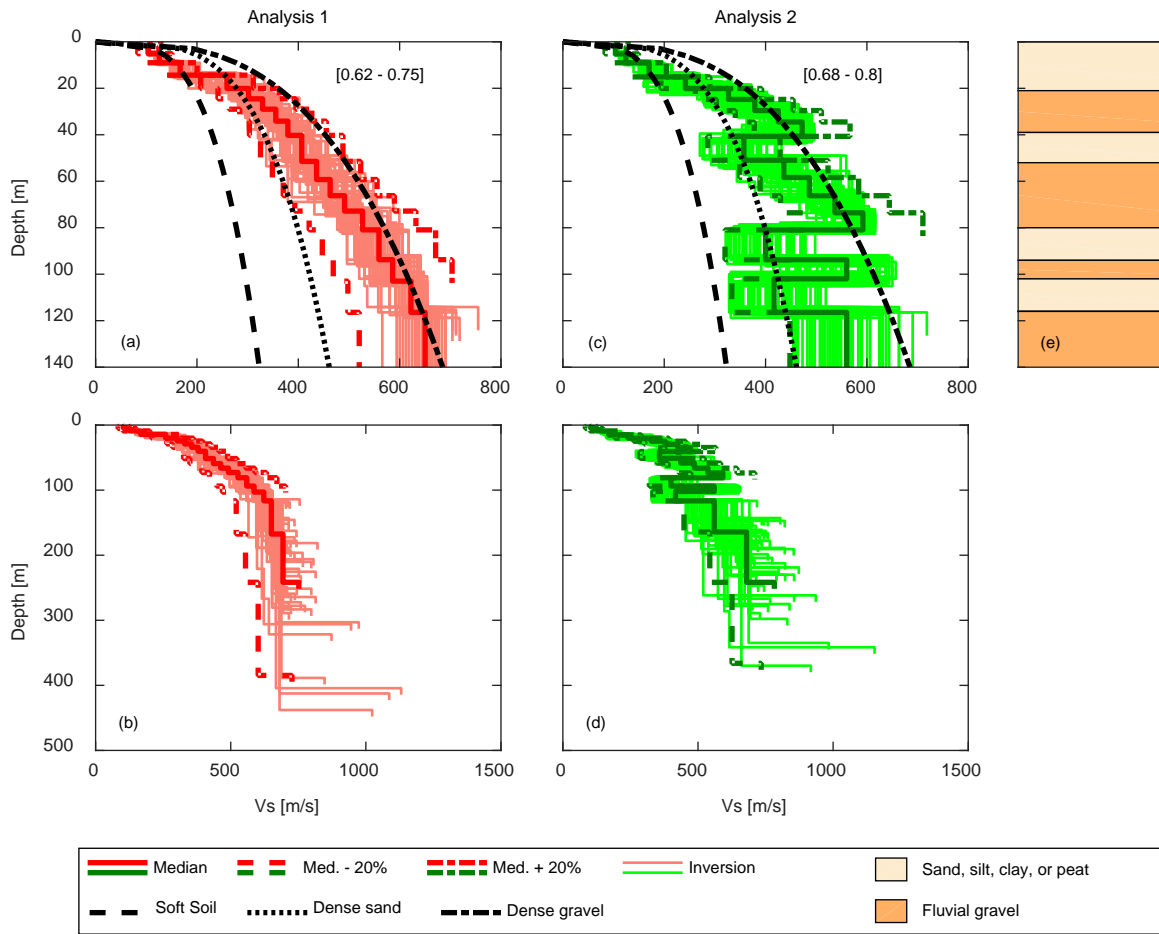


Fig. 1: Fifty Vs profiles chosen for site response analyses at Hagley Park from (a,b) Analysis 1 and (c,d) Analysis 2. Also shown are the median and +/-20% Vs profiles. Note that dispersion misfit values are indicated in brackets. The approximate geologic stratigraphy is shown in (e). Also shown are empirical reference Vs curves from Lin et al. 2014 for soft soil, dense sand, and dense gravel.

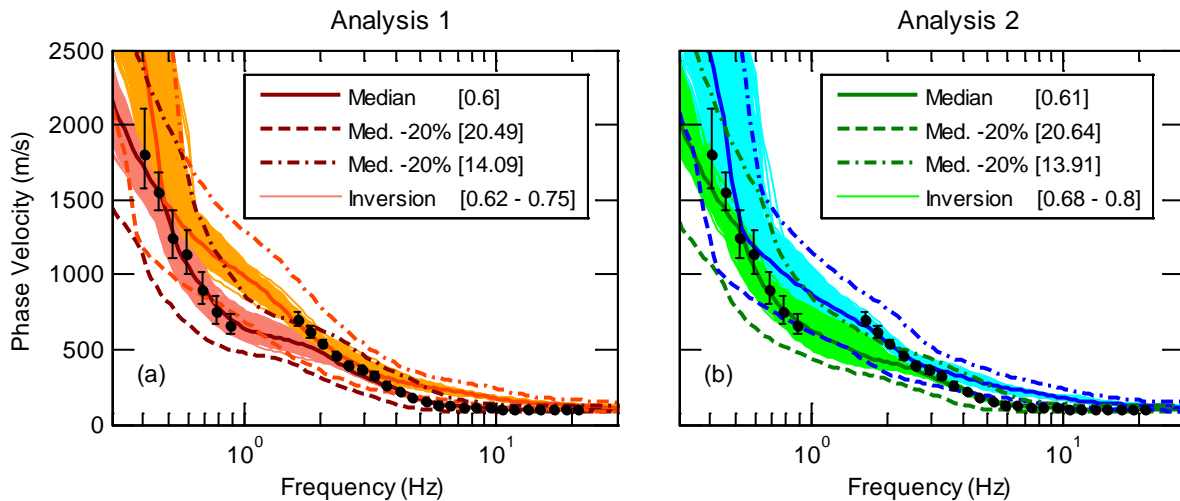


Fig. 2: Experimental dispersion data along with the theoretical dispersion data corresponding to the 50 Vs profiles chosen for site response analyses from (a) Analysis 1 and (b) Analysis 2. Also shown are the theoretical dispersion curves corresponding to the median and +/- 20% Vs profiles. Note that fundamental mode (red and



green) and first higher mode (orange and cyan) theoretical dispersion curves are shown. Dispersion misfit values are indicated in brackets.

computed from the 1,000 lowest misfit  $V_s$  profiles after the inversion was complete. For comparison purposes, theoretical dispersion curves were computed for these profiles. The computation of theoretical dispersion curves for these profiles required some assumptions regarding  $V_p$  and mass density. The assumptions made in this study were consistent with those described in Griffiths et al. (2016a) [13].

The median  $V_s$  profiles from Analyses 1 and 2 (see Fig. 1) capture the general trends of the  $V_s$  profiles that they were computed from. Moreover, the corresponding theoretical dispersion curves yield very low misfit values of 0.60 and 0.61, respectively. In fact, the misfit values associated with the median profiles are lower than any of the 50 profiles that came directly from either inversion and are essentially equal to the minimum misfits that were achieved for each analysis. (Note that due to the random sampling of the 1,000 lowest misfit profiles, the minimum misfit profile was not included in the set of 50 profiles for each analysis).

In contrast to the median profiles, theoretical dispersion curves for the  $\pm 20\%$  profiles (see Fig. 2) poorly match the experimental dispersion data and result in very high misfit values for both analyses. While these profiles appear reasonable when viewed with the  $V_s$  profiles coming directly from the inversion (see Fig. 1), the fact that their theoretical dispersion curves poorly match experimental dispersion data (i.e., misfit values ranging from approximately 14 – 20) indicates that these profiles fail to capture the “site signature”. Multiple studies have demonstrated that the experimental dispersion data can be robustly determined (e.g. Cox et al. 2014 [14], Garofalo et al. 2016 [15]). Moreover, since the experimental dispersion data contains valuable information regarding wave propagation across the site, it is worth considering whether  $V_s$  profiles that fail to capture this “site signature” are truly representative of the site.

### 3. Linear-Elastic Site Response

Linear-elastic acceleration transfer functions (TF) were computed for all 106  $V_s$  profiles shown in Fig. 2 (50 from inversion and a median and  $\pm 20\%$  profiles for each analysis). Small strain damping ratios ( $D$ ) were assigned using the relationships proposed by Darendeli (2001) [16]. Although these transfer functions are only valid for extremely small shear strains, they are not influenced by soil nonlinearity. Thus, they are useful for isolating the influence of the input  $V_s$  profile on the predicted surface response. Acceleration transfer functions for each  $V_s$  profile are shown in Fig. 3. Also shown is the experimentally measured horizontal-to-vertical (H/V) spectral ratio curve at the site. Similar to the experimental dispersion curve, the experimental H/V curve contains valuable information regarding small-strain wave propagation and site resonance. Studies have demonstrated that if an H/V curve exhibits a well-defined peak, then this peak approximately coincides with the fundamental shear wave resonant frequency of the site, although the magnitudes are poorly correlated (e.g., Lachet and Bard 1994 [17]). Thus, the H/V curve also represents a “signature” of the site. Therefore, it is useful to compare the theoretical linear-elastic shear wave transfer function to the experimental H/V curve. For both analyses, the fundamental shear wave resonant frequency is slightly higher than the measured H/V peak at 1.7 Hz. Nonetheless, the fundamental resonant frequencies for both analyses are generally within 1 Hz of the H/V peak, providing further evidence that the  $V_s$  profiles are reasonably capturing the “site signature.”

In an effort to better quantify the variability in the fundamental shear wave resonant frequency and its corresponding TF amplitude, box and whisker plots were created, as shown in Fig. 4. Note that box and whisker plots were created using the TFs associated with the 50  $V_s$  profiles derived directly from the inversions. While the resonant frequency and corresponding TF amplitude are shown for the median and  $\pm 20\%$  profiles, they were not used to compute the box and whisker plots. It is clear from Fig. 4a that the resonant frequencies associated with Analyses 1 and 2 exhibit comparable variability (roughly 1 Hz from the upper to lower whisker). However, despite a few outliers, resonant frequencies associated with Analysis 2 are lower and generally are in better agreement with the H/V peak. Nonetheless, the median resonant frequencies of 2.53 and 2.17 Hz, respectively, are within approximately 15% of one another. The resonant frequency associated with the median  $V_s$  profile (not to be confused with the median resonant frequency, computed from the TF of the 50  $V_s$  profiles derived directly from the inversion) coincides with the median value for both analyses, suggesting that it is a

reasonable representation of the profiles derived directly from the inversion. Conversely, the -20% profiles coincide with the lower whisker for each analysis and the +20% profiles exceed the upper whisker, suggesting that they do not capture the resonance features of the Vs profiles that they were computed from.

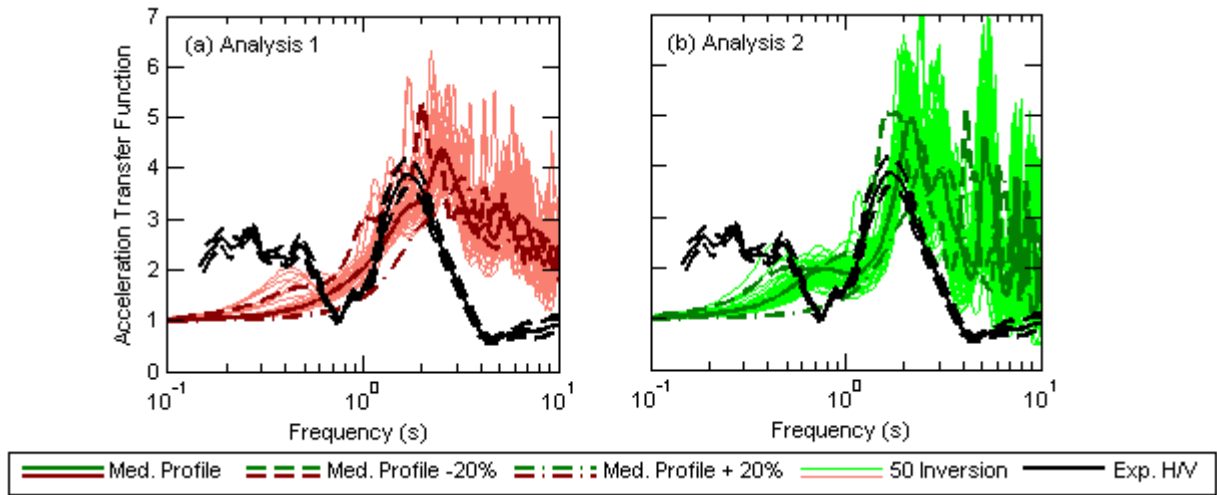


Fig. 3: Linear elastic transfer function corresponding to (a) Analysis 1 and (b) Analysis 2.

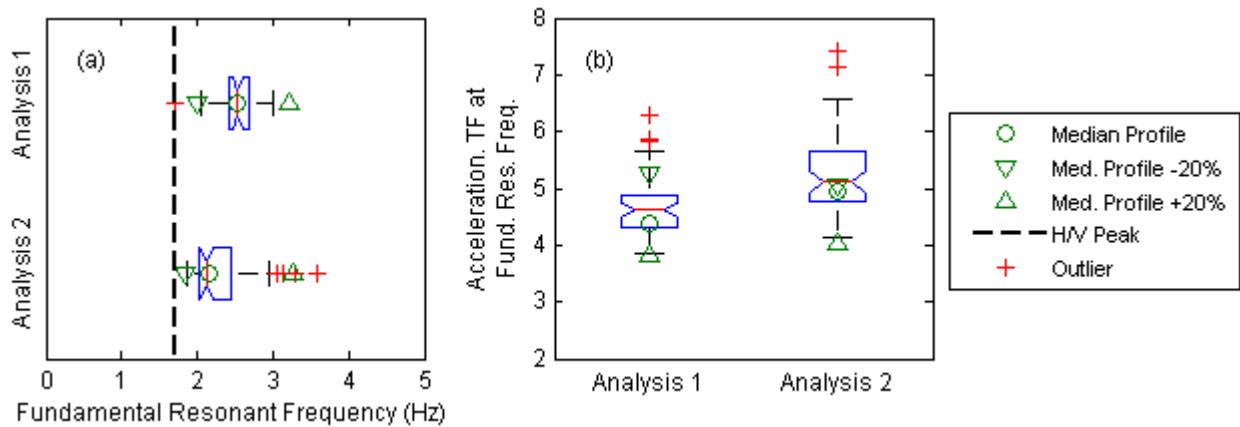


Fig. 4: Box-and-whisker plots for the (a) fundamental resonant frequency and (b) amplitude of transfer function at the fundamental resonant frequency for Analyses 1 and 2.

The TF amplitude at the resonant frequency is shown in Fig. 4b. It is clear that the TF amplitude at the resonant frequency is generally lower for Analysis 1 than Analysis 2, with median values of 4.61 and 5.12, respectively. The range in TF amplitude is also slightly higher for Analysis 2. Within each analysis, the TF amplitude associated with the median Vs profile lies between the first quartile and the median. TF amplitudes associated with the +20% profiles are below the lower whisker for both analyses, while the TF amplitudes associated with the -20% profiles are in reasonable agreement with the TF amplitudes of those profiles derived directly from the inversion. As mentioned earlier, all TF amplitudes are not influenced by soil-nonlinearity and thus damping ratios do not increase with shear strains.

#### 4. Equivalent-Linear Site Response

High- and low- intensity equivalent linear site response analyses were performed on all 106 Vs profiles shown in Fig. 2. The Boore and Atkinson (2008) [18] ground motion prediction equation (GMPE) was used to develop a





target spectrum for the selection of appropriate input rock ground motions (GMs). The target was computed using the following assumptions: a moment magnitude ( $M_W$ ) of 7.5, a Joyner-Boore distance ( $R_{JB}$ ) of 15 km, and an average  $V_s$  in the top 30 m ( $V_{S30}$ ) of 760 m/s. A library of 80 candidate time histories recorded at sites with  $V_{S30}$  between 500 and 1500 m/s,  $R_{JB}$  between 5 km and 80 km, and  $M_W$  between 7.0 and 8.0 was developed using the PEER NGA West database. The SigmaSpectra software (Kottke and Rathje 2012 [19]) was used to select and scale seven ground motions that, on average, matched the shape and amplitude of the target response spectrum. In an effort to observe the influence of earthquake intensity, the input ground motions were re-scaled in order to obtain average peak ground accelerations (PGA) of 0.05 and 0.30 g. These ground motions are referred to herein as “low-intensity” and “high-intensity”, respectively.

Equivalent-linear analyses were performed in Matlab using codes that were developed at the University of Texas (George Zalachoris, personal communication, 2014). These codes divided major layers into sub-layers so that numerical filtering below 50 Hz would not be problematic. Analyses were performed in batch mode, looping through sets of candidate  $V_s$  profiles using seven GMs per profile. This code has been verified in the past by comparing amplification factors and pseudo-acceleration response spectra with those computed in DEEPSOIL v5.1 (Griffiths et al. 2016b [8]). Non-linear soil properties were assigned using the depth/confining pressure-dependent normalized modulus reduction ( $G/G_{max}$ ) and damping ( $D$ ) relationships proposed by Darendeli (2001) [16]. In an effort to isolate the influence of the input  $V_s$  profile, all layers were assumed to be non-plastic ( $PI = 0$ ) and normally-consolidated ( $OCR = 1$ ).

#### 4.1 Low-Intensity Input Ground Motions

The response spectra (RS) associated with the low-intensity input ground motions (scaled to an average PGA of 0.05 g) are shown in Fig. 5. Note that one response spectrum is shown for each  $V_s$  profile, which represents the median of the response spectra corresponding to the seven input ground motions. RS associated with the inversion  $V_s$  profiles from Analysis 2 exhibit slightly more variability than those from Analysis 1. However, both sets of response spectra are tightly grouped and exhibit relatively low variability. Both analyses show spectral accelerations (SA) in excess of 0.2 g between 0.2 and 0.6 s. Predominant periods for both analyses are generally between 0.25 and 0.5 s.

Spectral accelerations associated with the median profiles (thick solid lines in Fig. 5) fall within the range defined by the 50 inversion profiles (thin solid lines in Fig. 5), although they are at the higher end of the range in both cases. Spectral accelerations associated with the +20% profiles are slightly higher than those of the 50 inversion profiles for both analyses, yet still represent a reasonable upper-bound. Conversely, the SA associated with the -20% profile is significantly lower than the SA associated with all other profiles in Analysis 1, and thus is a poor lower-bound. The SA associated with the -20% profile from Analysis 2 appears to be a more reasonable lower-bound for that analysis.

In order to directly compare the low-intensity site response predictions from Analyses 1 and 2, a lognormal median and +/- one standard deviation response spectra, transfer function, and shear strain profile were computed using the results from the 50 inversion  $V_s$  profiles from each analysis. The results are shown in Fig. 6. Despite major differences in the  $V_s$  profiles from each analysis (refer to Fig. 1), the median response spectra and transfer functions are remarkably similar. Moreover, the proximity of the lognormal median to the +/- one standard deviation curves underscores the minimal variability in the predicted response spectra and transfer functions from both analyses.

Fig. 6c shows the maximum shear strain profiles for both analyses. Shear strains associated with Analysis 2 are lower in the gravel formations (20 to 40 m and 55 to 80 m, see Fig. 1) and higher in the marine sands, silts, and clays (40 to 55 m and 80 to 95 m, see Fig. 1). This is because  $V_s$  profiles derived from Analysis 2 accounted for material type and were relatively stiff (high  $V_s$  values) in the gravel and relatively soft (low  $V_s$  values) in the marine sands, silts, and clays. Conversely,  $V_s$  profiles derived from Analysis 1 essentially averaged material types. Nonetheless, the maximum shear strain at the ground surface is extraordinarily similar in both cases with an amplitude of approximately  $5 \times 10^{-3}\%$ .

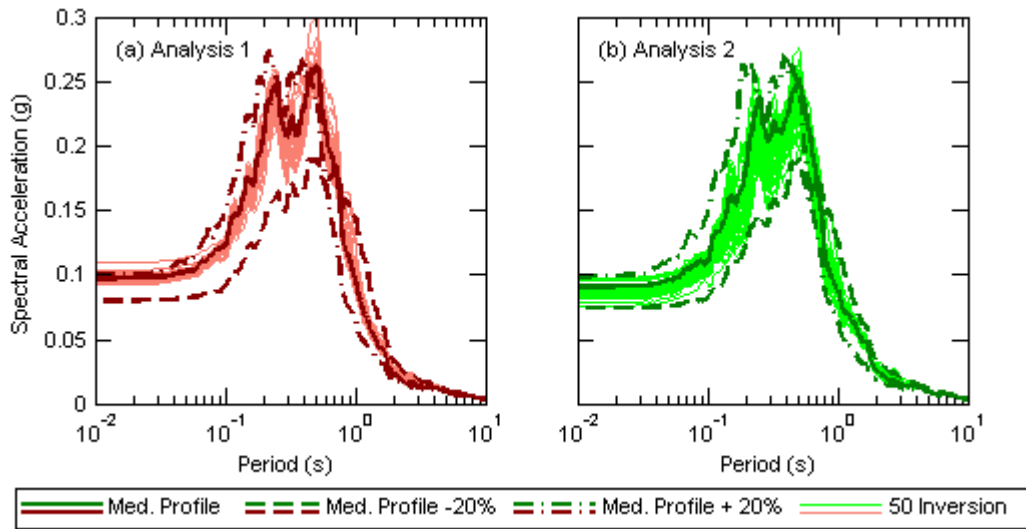


Fig. 5: Median response spectra obtained from low-intensity equivalent-linear site response analyses using a suite of seven input ground motions scaled to an average PGA of 0.05 g and Vs profiles corresponding to (a) Analysis 1 and (b) Analysis 2.

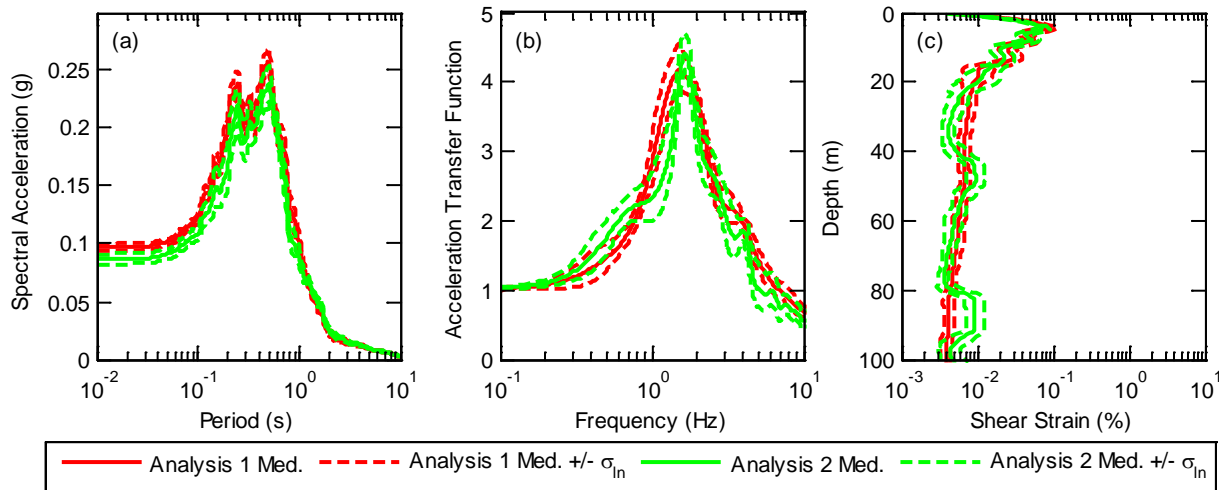


Fig. 6: Lognormal median and +/- one standard deviation (a) response spectra, (b) transfer function, and (c) maximum shear strain profile corresponding to low-intensity input ground motions for Vs profiles from Analyses 1 and 2. Note that each response spectrum, transfer function, and strain profile used to compute the median +/- one standard deviation was itself a median, computed using seven input ground motions scaled to an average PGA of 0.05 g.

#### 4.2 High-Intensity Input Ground Motions

The response spectra associated with the high-intensity input ground motions (scaled to an average PGA of 0.30 g) are shown in Fig. 7. One response spectrum, which represents the median RS of all seven input GMs, is shown for each Vs profile. The response spectra for the 50 inversion Vs profiles are tightly grouped for both analyses. Similar to the low-intensity input GMs, spectral accelerations associated with the median profile (thick solid lines in Fig. 7) fall within the range of the 50 inversion profiles (thin solid lines in Fig. 7), albeit on the higher end of the range. Conversely, response spectra associated with the +/-20% profiles are significantly higher/lower than all other profiles. These differences in spectral acceleration are much more significant than for the case of low-intensity input GMs (refer to Fig. 5). This underscores the influence of the larger shear strains induced by the high-intensity GMs and resulting soil nonlinearity.



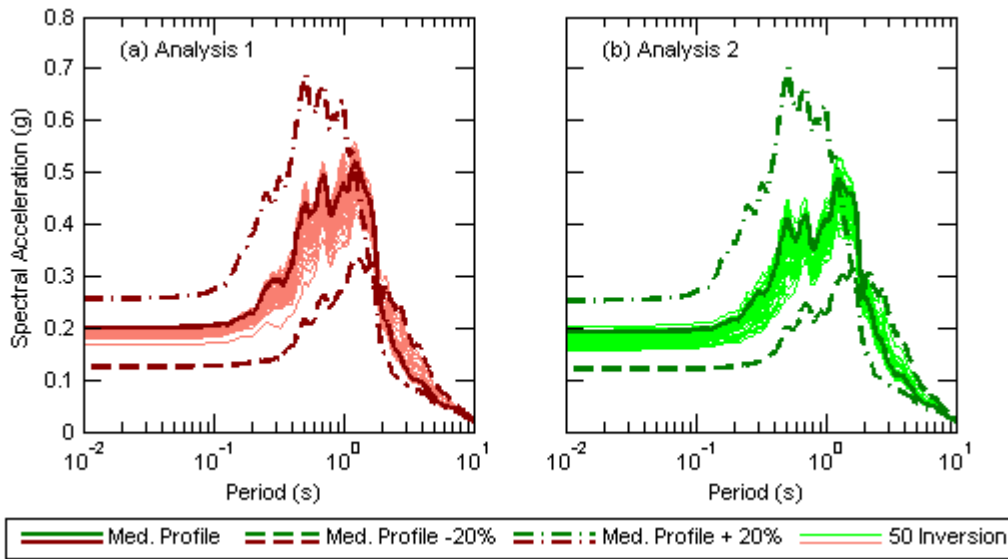


Fig. 7: Median response spectra obtained from high-intensity equivalent-linear site response analyses using a suite of seven input ground motions scaled to an average PGA of 0.30 g and Vs profiles corresponding to (a) Analysis 1 and (b) Analysis 2.

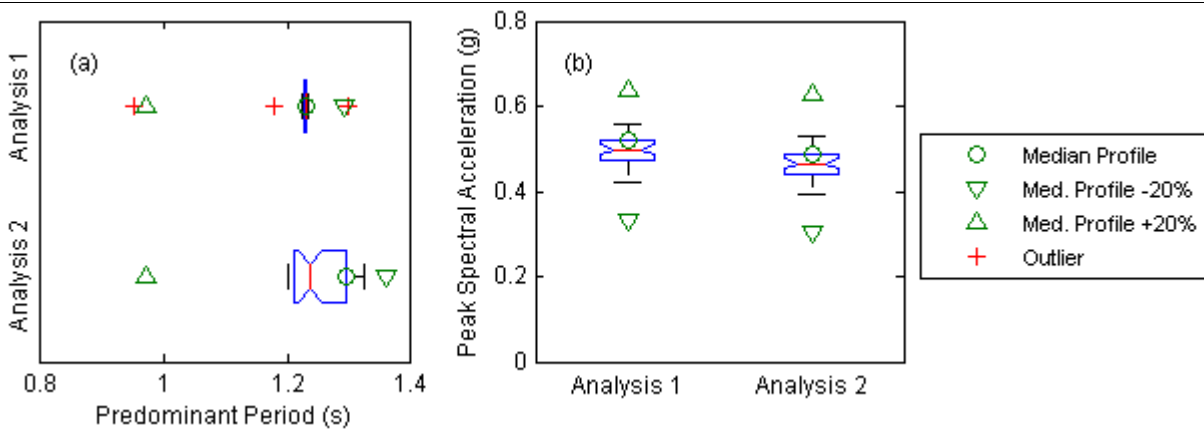


Fig. 8: Box-and-whisker plots for the (a) predominant period and (b) peak spectral acceleration (corresponding to the predominant period) for Analyses 1 and 2.

In an effort to better quantify the variability in the high-intensity response spectra, box and whisker plots were created for the predominant period and associated spectral acceleration, as shown in Fig. 8. Similar to the box and whisker plots shown in Fig. 4, box and whisker plots were created using only the response spectra associated with the 50 Vs profiles derived directly from the inversion. However, the predominant periods and spectral accelerations associated with the median and +/- 20% Vs profiles are shown for reference.

With the exception of three outliers, the response spectra associated with all inversion Vs profiles from Analysis 1 exhibit essentially the same predominant period. Conversely, predominant periods associated with Analysis 2 exhibit more variability, with values ranging from 1.20 to 1.32. These results differ from the linear elastic transfer functions (see Fig. 4), where the results from Analyses 1 and 2 exhibit similar variability. However, it is clear from Fig. 8a that the high-intensity median predominant periods for Analyses 1 and 2 are quite similar, with values of 1.23 and 1.24 s, respectively. Thus, while the predominant periods associated with the normally dispersive Vs profiles (Analysis 1) exhibit less variability than those associated with the Vs profiles that incorporate strong velocity reversals (Analysis 2), both sets of profiles yield similar estimates for predominant period. The predominant period associated with the median Vs profile (not to be confused with the

median predominant period, computed using the response spectra of the 50 inversion Vs profiles) is in the third quartile of the range defined by the 50 inversion Vs profiles for both analyses. Conversely, predominant periods associated with the +/-20% profiles are far outside of the whiskers.

Box and whisker plots for the spectral acceleration associated with the predominant period are shown in Fig. 8b. The range in peak SA for the 50 inversion profiles is approximately 0.14 g in both cases. However, peak spectral accelerations associated with Analysis 1 are slightly higher than those associated with Analysis 2, with medians of 0.50 g and 0.47 g, respectively. Nonetheless, these medians are within roughly 6 percent of one another. Given the major differences in the input Vs profiles from Analyses 1 and 2, this is quite remarkable. The peak SA associated with the median Vs profile is in the third quartile defined by the 50 inversion profiles for both analyses. Conversely, the peak SA associated with the +/-20% profiles are far above/below the whiskers for both analyses. It is worth reiterating that the +/-20% profiles also resulted in a poor fit of the experimental dispersion data and the fundamental shear wave resonant frequency generally did not match the H/V peak. Thus, these Vs profiles fail to capture the site signature and it is worth considering whether the variability that they exhibit is realistic or an artifact of including inappropriate Vs profiles in the site response calculations.

In order to directly compare the high-intensity site response predictions from Analyses 1 and 2, a lognormal median and +/- one standard deviation response spectra, transfer function, and shear strain profile were computed using the results from the 50 inversion Vs profiles from each analysis. The results are shown in Fig. 9a, 9b, and 9c, respectively. Spectral accelerations associated with Analysis 2 (strong velocity reversals included in the input Vs profiles) are slightly lower than those associated with Analysis 1 (normally dispersive input Vs profiles). Even still, spectral accelerations are generally in satisfactory agreement, with a maximum difference of about 20% at a period of 0.7 s. Similarly, the acceleration transfer functions are remarkably similar for Analyses 1 and 2. As for the low-intensity input ground motions, the maximum shear strain profiles exhibit significant differences at depth. Again the shear strains are lower in the gravel formations (20 to 40 m and 55 to 80 m) and higher in the marine sands, silts, and clays (40 to 55 m and 80 to 95 m) for Analysis 2. Nonetheless, maximum shear strains at the ground surface are in excellent agreement for both analyses with an amplitude of approximately 10<sup>-2</sup>%.

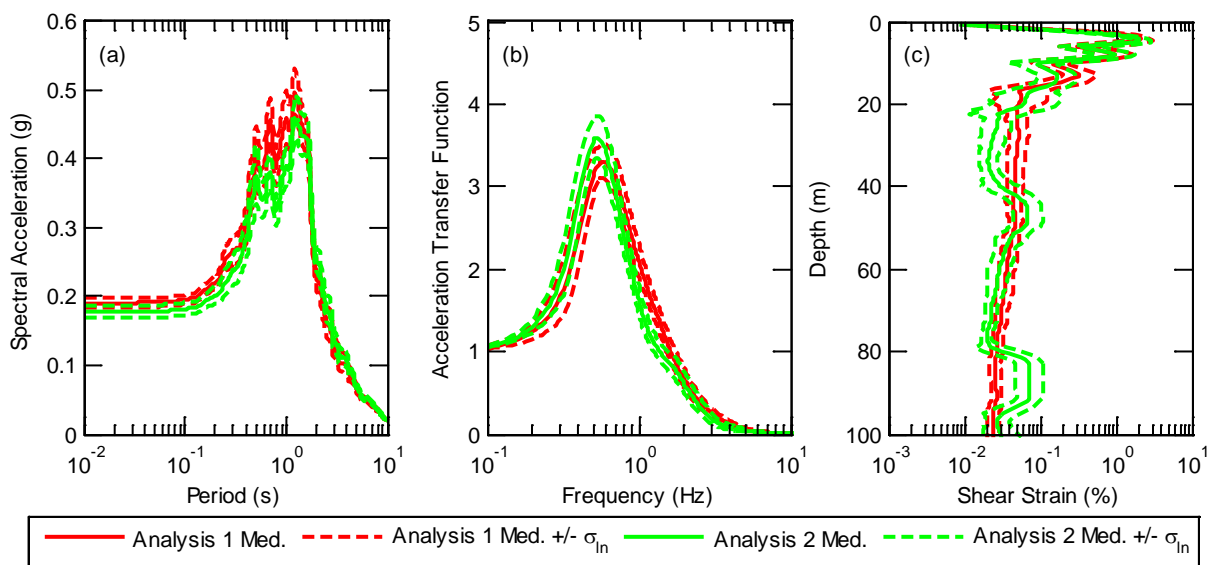


Fig. 9: Lognormal median and +/- one standard deviation (a) response spectra, (b) transfer function, and (c) maximum shear strain profile corresponding to high-intensity input ground motions for Vs profiles from Analyses 1 and 2. Note that each response spectrum, transfer function, and strain profile used to compute the median +/- one standard deviation was itself a median, computed using seven input ground motions scaled to an average PGA of 0.30 g.



## 5. Conclusions

Linear-elastic and equivalent-linear site response analyses were performed on two significantly different sets of Vs profiles, both of which were derived from the same experimental surface wave dataset. The first set of Vs profiles, Analysis 1, was developed blindly using normally dispersive inversion parameters that did not account for the complex local geology. The second set of Vs profiles, Analysis 2, incorporated strong velocity reversals where marine sands, silts, and clays were known to reside below stiffer alluvial gravels. The influence of the presence or lack of these velocity contrasts on the predicted site response is of interest. Thus, 50 Vs profiles were randomly sampled from the 1,000 lowest misfit profiles of each inversion analysis and used in subsequent site response analyses. Additionally, the median of the 1,000 lowest misfit profiles and “bounding-type” Vs profiles (i.e., the median Vs profile with +/- 20% applied to Vs) were considered.

Linear-elastic transfer functions corresponding to Vs profiles derived directly from each inversion were in reasonable agreement. The fundamental shear wave resonant frequencies associated with Analysis 2 were slightly lower than those associated with Analysis 1. However, the median resonant frequencies of both analysis were within approximately 15% of one another. The TF associated with the median Vs profile (not to be confused with the median TF) captures the resonance features demonstrated by the 50 inversion Vs profiles. Conversely, the +/-20% profiles exhibit significantly stiffer/softer responses than all other profiles.

Overall, the equivalent-linear site response analyses yielded similar results for both sets of Vs profiles. Both the response spectra and transfer functions were in excellent agreement for both low- and high-intensity input ground motions. While the maximum shear strain profiles showed significant differences at depth, shear strains at the ground surface were essentially identical. Similar to the linear-elastic case, site response predictions corresponding to the median Vs profile are in agreement with those corresponding to the inversion Vs profiles. Site response predictions associated with the +/-20% profiles are in fair agreement with all other profiles for the low intensity input GMs. However, as the ground motion intensity increases, the predicted site response associated with these profiles becomes substantially stiffer/softer than all other profiles. It should be noted that the forward-computed theoretical dispersion curves for the +/-20% profiles poorly matched the experimental dispersion data, suggesting that these profiles are not the best candidates for use in site response. On the other hand, all Vs profiles whose theoretical dispersion data satisfactorily fit the experimental dispersion data yielded similar response spectra, transfer functions, and shear strains at the ground surface, regardless of whether or not they included velocity reversals. These findings need to be confirmed at additional sites with inverse velocity layers covering a broad range of geologic conditions before we can confidently conclude that site response estimates based on normally dispersive Vs profiles and those with strong velocity reversals are quite similar so long as the Vs profiles fit the experimental site signature (i.e., the experimental dispersion data and H/V curves).

## 5. Acknowledgements

This work was supported primarily by U.S. National Science Foundation (NSF) grant CMMI-1261775. However, any opinions, findings, and conclusions or recommendations expressed in this material are those of the authors and do not necessarily reflect the views of NSF. Financial support from the N.Z. Earthquake Commission (EQC) is also acknowledged and greatly appreciated. Any opinions, findings, and conclusions or recommendations expressed in this material are those of the authors and do not necessarily reflect the views of the Consortium of Organizations for Strong-Motion Observation Systems (COSMOS) Facilitation Committee for the Development of the COSMOS International Guidelines for the Application of Non-Invasive Geophysical Techniques to Characterize Seismic Site Conditions.

## 6. References

- [1] American Association of State Highway and Transportation Officials (AASHTO): *Guide Specifications for LRFD Seismic Bridge Design 2011*. 2nd ed., published by AASHTO, Washington, D.C.
- [2] American Society of Civil Engineers (ASCE): *Minimum design loads for buildings and other structures*, ASCE Standard ASCE/SEI 7-10, published by ASCE, Reston, Virginia.



- [3] Matasovic, N., and Hashash, Y. (2012): NCHRP Synthesis 428: Practices and Procedures for Site Specific Evaluations of Earthquake Ground Motions, A Synthesis of Highway Practice. *National Cooperative Highway Research Program of the Transportation Research Board*, Washington, D.C.
- [4] DiGiulio, G., Savvaidis, A., Ohrnberger, M., Wathelet, M., Cornou, C., Knapmeyer-Endrun, B., Renalier, F., Theodoulidis, N., and Bard, P.Y. (2012): Exploring the model space and ranking a best class of models in surface-wave dispersion inversion: Application at European strong-motion sites. *Geophysics*, **77** (3), B147–B166.
- [5] Cox, B.R. and Teague, D.P. (2016): Layering Ratios: A Systematic Approach to the Inversion of Surface Wave Data in the Absence of A-priori Information. *Geophysical Journal International*, **207** (1), 422–438.
- [6] Foti, S., Comina, C., Boiero, D., and Socco, L.V. (2009): Non-uniqueness in surface-wave inversion and consequences on seismic site response analyses. *Soil Dynamics and Earthquake Engineering*, **29**, 982–993.
- [7] Boaga, J., Vignoli, G., and Cassiani, G. (2011): Shear wave profiles from wave surface inversion: the impact of uncertainty on seismic site response analysis. *Journal of Geophysics and Engineering*. **8**, 162-174.
- [8] Griffiths, S.C., Cox, B.R., Rathje, E.M., Teague, D.P. (2016). Mapping Dispersion Misfit and Uncertainty in Vs Profiles to Variability in Site Response. *Journal of Geotechnical and Geoenvironmental Engineering*, DOI: 10.1061/(ASCE)GT.1943-5606.0001553.
- [9] Teague, D.P. and Cox, B.R. (2016): Site Response Implications Associated with using Non-Unique Vs Profiles from Surface Wave Inversion in Comparison with Other Commonly Used Methods of Accounting for Vs Uncertainty. *Soil Dynamics and Earthquake Engineering*, <http://dx.doi.org/10.1016/j.soildyn.2016.07.028>.
- [10] Brown, L.J., Wilson, D.D., Moar, N.T., and Mildenhall, D.C. (1988): Stratigraphy of the late Quaternary deposits of the northern Canterbury Plains, New Zealand. *NZ J. of Geology and Geophysics*, **31**, 305-335.
- [11] Teague, D., Cox, B., Bradley, B., and Wotherspoon, L.M. (2015): Development of Realistic Vs Profiles in Christchurch, New Zealand via Active and Ambient Surface Wave Data: Methodologies for Inversion in Complex Interbedded Geology. *Proc. of the 6th International Conference on Earthquake Geotechnical Engineering*, Christchurch, New Zealand.
- [12] Lin, Y., Joh. S., and Stokoe, K. (2014). Analyst J: Analysis of the UTexas 1 Surface Wave Dataset Using the SASW Methodology. *ASCE Geo-Congress 2014: Geo-Characterization and Modeling for Sustainability*, Atlanta, Georgia, United States.
- [13] Griffiths, S.C., Cox, B.R., Rathje, E.M., Teague, D.P. (2016a): A Surface Wave Dispersion Approach for Evaluating Statistical Models that Account for Shear Wave Velocity Uncertainty. *Journal of Geotechnical and Geoenvironmental Engineering*, DOI: 10.1061/(ASCE)GT.1943-5606.0001552.
- [14] Cox, B.R., Wood, C.M., and Teague, D.P. (2014): Synthesis of the UTexas1 Surface Wave Dataset Blind-Analysis Study: Inter-Analyst Dispersion and Shear Wave Velocity Uncertainty,” *ASCE Geo-Congress 2014: Geo-Characterization and Modeling for Sustainability*, Atlanta, GA.
- [15] Garofalo, F., Foti, S., Hollender, F., Bard, P.Y., Cornou, C., Cox, B.R., Ohrnberger, M., Sicilia, D., Asten, M., Di Giulio, G., Forbriger, T., Guillier, B., Hayashi, K., Martin, A., Matsushima, S., Mercerat, D., Poggin, V., & Yamanaka, H. (2016a). “Interpacific project: comparison of invasive and non-invasive methods for site characterization. Part I: Intra-comparisson of surface wave methods.” *Soil Dynamics and Earthquake Engineering*, **82**, 222–240, doi:10.1016/j.soildyn.2015.12.010.
- [16] Darendeli, M.B. (2001). *Development of A New Family of Normalized Modulus Reduction and Material Damping Curves*. Ph.D. Dissertation, School of Civil, Architectural and Environmental Engineering, The University of Texas at Austin, Austin, TX.
- [17] Lachet, C. and Bard, P.-Y. (1994). Numerical and theoretical investigations on the possibilities and limitations of Nakamura’s technique. *Journal of Physics of the Earth*, **42**, 377–397.
- [18] Boore, D., and G. Atkinson (2008). Ground-motion Prediction Equations for the Average Horizontal Component of PGA, PGV, and the 5%-damped PSA at spectral periods between 0.01 s and 10.0 s. *Earthquake Spectra*, **24**, 99-138.
- [19] Kottke, A. and Rathje, E. (2012): *Technical Manual for SigmaSpectra*. <<http://nees.org/resources/sigmaspectra>>